

Structure and Aggregation of a Helix-Forming Polymer

James E. Magee, Zhankai Song, Robin A. Curtis, and Leo Lue

*School of Chemical Engineering and Analytical Science, The University of Manchester,
PO Box 88, Sackville Street, Manchester, M60 1QD, United Kingdom*

We have studied the competition between helix formation and aggregation for a simple polymer model. We present simulation results for a system of two such polymers, examining the potential of mean force, the balance between inter and intramolecular interactions, and the promotion or disruption of secondary structure brought on by the proximity of the two molecules. In particular, we demonstrate that proximity between two such molecules can stabilize secondary structure. However, for this model, observed secondary structure is not stable enough to prevent collapse of the system into an unstructured globule.

I. INTRODUCTION

Aggregation of partially folded proteins is a problem in many bio-related fields. In bioprocessing operations, mechanical and/or environmental stresses lead to protein unfolding which may result in irreversible aggregation and loss of protein activity.¹ Another problem in bioprocessing is the recovery of partially-folded recombinant proteins, produced in densely packed “inclusion bodies”. Recovery of these proteins requires dissolving the bodies in denaturant and then slowly diluting the solution, minimizing unwanted aggregation such that the protein folds to the native state. Finally, protein aggregation has been implicated in the origin of amyloid fibrils, which have been linked to many different diseases.^{2,3,4} Understanding the process of aggregation, and determining the conditions under which it will take place, is therefore a matter of some importance.

The competition between protein folding and protein aggregation is believed to be determined by the balance of inter and intramolecular forces. Protein folds are stabilized by strong intramolecular interactions between hydrophobic and hydrogen bonding groups in the protein interior. Aggregation of folded proteins is of necessity weak, mediated by interactions between heavily solvated charged and polar surface groups. However, at high temperatures, or upon addition of denaturant, the fold becomes less stable. This structural disruption causes hydrogen bonding and hydrophobic groups to become exposed, providing “sticky” sites for aggregation. The resulting competition between structure formation and aggregation may hold the key to understanding the process of aggregation.

The details of this process are difficult to experimentally resolve, since partially folded intermediates have very low solubilities. As such, computational approaches are extremely useful. Detailed, all-atom models have been used to study the process of aggregation.^{5,6,7,8,9} However, such models are computationally intensive, and details of the force field used can cloud underlying behavior. Simple “reduced models” that can produce protein-like secondary structure^{10,11,12,13,14,15,16,17,18} are therefore useful as a parallel approach to the problem.

In a previous paper,¹⁹ we proposed an isotropic polymer model which can form helical secondary structure. This model consists of a chain of overlapping spherical beads, and is related to the well-studied tangent-sphere square-well polymer chain model. Low temperature transitions to “crystalline” ordered states have been observed for tangent sphere polymers^{20,21,22} Further, interactions between pairs of tangent-sphere polymers are well studied.²³

In this paper, we extend the study of the overlapping bead model by examining the behavior of isolated pairs of such polymers. In particular, we examine how the formation of helical structure affects the interactions between the two molecules and influences the structure of the resulting complex. The remainder of this paper is organized as follows. In section II, we describe the simulation methodology and the particulars of the model. In section III, we present the results from the simulations, and in section IV, we present our conclusions.

II. SIMULATION DETAILS

The polymer model we consider consists of a linear chain of N impenetrable spheres of diameter σ . The distance between bonded spheres is restricted to vary between $0.9l$ and $1.1l$, where l is the nominal bond length. Directly bonded spheres may overlap (i.e., $\sigma > l$), although non-bonded spheres may not. In addition to excluded volume interactions, the spheres also interact via a square-well potential. The interaction potential $u(r)$ between the spheres is given by:

$$u(r) = \begin{cases} \infty & \text{for } r < \sigma \\ -\epsilon & \text{for } \sigma < r < \lambda\sigma \\ 0 & \text{for } \lambda\sigma < r \end{cases} \quad (1)$$

Table I: Temperatures used in simulations.

Box	$\beta\epsilon$	$k_B T/\epsilon$	Box	$\beta\epsilon$	$k_B T/\epsilon$
1	0.18014	5.55112	11	1.53610	0.65100
2	0.22518	4.44089	12	1.76056	0.56800
3	0.28147	3.55271	13	2.01207	0.49700
4	0.35184	2.84217	14	2.29885	0.43500
5	0.43980	2.27374	15	2.62467	0.38100
6	0.54976	1.81899	16	3.00300	0.33300
7	0.68719	1.45519	17	3.43643	0.29100
8	0.85899	1.16415	18	3.92157	0.25500
9	1.07374	0.93132	19	4.50450	0.22200
10	1.34218	0.74506	20	5.12821	0.19500

where r is the distance between the centers of the spheres, ϵ is the strength of the square-well interaction, and λ characterizes the width of the square-well interaction. In this work, $\lambda = 1.5$. Since this potential is pairwise, the interaction energy of a system of polymers can be decomposed into an intramolecular energy E_{intra} (interactions between monomers on the same molecule) and an intermolecular energy E_{inter} (interactions between monomers on different molecules). At $\sigma/l = 1.0$, the model reduces to the traditional tangent sphere polymer model; interactions between pairs of such polymers has been studied extensively elsewhere.^{23,24,25,26,27} For larger values of σ/l , we have observed helix formation,¹⁹ despite the isotropic, achiral nature of the model. While the precise mechanism of helix formation for this model remains unclear, it has been suggested that helices are in fact the optimal packing structure for any string-like object,²⁸ in the same fashion that optimal packing of spheres yields hexagonal or cubic close-packed periodic lattices.

Monte Carlo simulations were performed for a pair of $N = 20$ (20mer) square-well molecules with $\sigma/l = 1.3, 1.6$, and 1.9 . Pivot, crank-shaft, and sphere displacement moves were used to sample the individual polymer conformations. Overall translation and rotation moves of the polymers were performed to sample the relative positions and orientations of the polymers. Umbrella sampling of the polymer separation was performed with a potential of the form

$$U(r) = a(r - b)^2 \quad (2)$$

where r is the center of mass separation between the polymers, and the parameter $a = 40k_B T$ was used to sample intervals in polymer center of mass separation. The parameter b was varied from a value of 0 to $25l$. The values of b were initially distributed evenly in units of l , and extra values were added wherever insufficient overlap in r histograms was observed. For each umbrella potential, parallel tempering in temperature was used to enhance equilibration of the low temperature systems. The temperatures used in the simulations are given in Table I. For each umbrella potential, the multiple histogram method was used to combine simulation data at different temperatures.

Each production simulation run consisted of a total of 10^6 parallel tempering (box swap) moves. Between each of these attempted moves, 80 pivot, crank-shaft, and sphere displacement moves were attempted, as well as 80 molecular translation and rotation moves. Samples of the system configuration were taken after every 10^3 attempted parallel tempering moves. For each set of conditions, an equilibration run of 10^5 attempted parallel tempering moves was performed, followed by 10 production runs. The reported results are averages over the production runs, and the uncertainties were estimated by the jackknife method.

We are particularly interested in the influence of intermolecular interactions on the helical structure which has been observed for this model in isolation.¹⁹ As such, structures are characterized through the torsion τ . For a continuous space curve $\mathbf{R}(s)$, the torsion is defined as:

$$\tau(s) = \frac{(\mathbf{R}'(s) \times \mathbf{R}''(s)) \cdot \mathbf{R}'''(s)}{|\mathbf{R}'(s) \times \mathbf{R}''(s)|^2} \quad (3)$$

where primes denote derivatives with respect to s . For the polymer chain, the required derivatives are calculated

using a central difference approximation:

$$\begin{aligned}\mathbf{R}'_i &= \frac{1}{2}(\mathbf{R}_{i+1} - \mathbf{R}_{i-1}) \\ \mathbf{R}''_i &= \mathbf{R}_{i+1} - 2\mathbf{R}_i + \mathbf{R}_{i-1} \\ \mathbf{R}'''_i &= \frac{1}{2}(\mathbf{R}_{i+2} - 2(\mathbf{R}_{i+1} - \mathbf{R}_{i-1}) - \mathbf{R}_{i-2})\end{aligned}\quad (4)$$

where \mathbf{R}_i is the vector position of monomer i . An instantaneous molecular conformation is characterized by the configurational average torsion $\bar{\tau}$, given by:

$$\bar{\tau} = \bar{\tau} = \sum_{i=3}^{N-2} \tau_i / (N-4) \quad (5)$$

where τ_i is the torsion at monomer i , defined on $i \in [3, N-2]$, and the bar denotes an instantaneous configurational average. Chiral (torsional) symmetry breaking is used to detect helix structure formation; helix formation is associated with a probability distribution $p(\bar{\tau})$ which is bimodal, symmetric, and with $p(\bar{\tau} = 0) \approx 0$. Combined with observation of helical snapshot configurations, this provides strong evidence for helicity. Structures are also characterized by the absolute of the mode of $p(\bar{\tau})$, denoted $\bar{\tau}_{max}$.

It is also instructive to consider statistical correlations between properties of the molecules. The correlation between observables \mathcal{A} and \mathcal{B} is given by:

$$\text{cor}(\mathcal{A}, \mathcal{B}) = \frac{(\langle \mathcal{A} \mathcal{B} \rangle - \langle \mathcal{A} \rangle \langle \mathcal{B} \rangle)^2}{(\langle \mathcal{A}^2 \rangle - \langle \mathcal{A} \rangle^2)(\langle \mathcal{B}^2 \rangle - \langle \mathcal{B} \rangle^2)} \quad (6)$$

where angle brackets denote ensemble averaging. A correlation of zero indicates that the two variables are completely uncorrelated, while a correlation of one indicates perfect linear correlation. We measure correlations between the intramolecular energies of the individual molecules $\text{cor}(E_{intra}^{(1)}, E_{intra}^{(2)})$, the torsions of the individual molecules $\text{cor}(\bar{\tau}_1, \bar{\tau}_2)$, and the orientations of the end-to-end bond vectors, $\langle |\hat{\mathbf{r}}_{e(1)} \cdot \hat{\mathbf{r}}_{e(2)}| \rangle$. The last quantity should take a value of one if the end-to-end vectors of the molecules are aligned, zero if the end-to-end vectors are perpendicular, and a half if the orientations are uncorrelated. The absolute value of the dot product is taken because the molecules have no directionality; antiparallel orientations are equivalent to parallel orientations. For unstructured globules, we expect this quantity to be one half (since the end-to-end vector should be randomly oriented), whereas for helical structures, the end-to-end vectors are a reasonable approximation for the helical axes, and the dot product provides a measure of the orientational correlation of the helices.

The pair potential of mean force (PMF) $\psi(r)$ is estimated from the observed histograms $h(r)$ of separation between molecules. For a given simulation, this is given by:

$$\psi(r) = -k_B T \ln(h(r)/r^2) - U(r) + C \quad (7)$$

where k_B is the Boltzmann constant and C is an unknown energy offset, arising from the incomplete normalization of probability histograms from simulation. The $U(r)$ term removes the bias introduced by the umbrella potentials. Since solvent is implicit, $\psi(r) = 0$ at separations for which the polymers can have no direct interaction (i.e., $r/l > (N-1) + \lambda\sigma/l$). For simulations sampling these large values of r , it is possible to fix C by this criterion. Results for neighboring umbrellas are then “patched” together by finding values for C which minimize the total statistical uncertainty in the combined results.

The last quantity of interest is the second virial coefficient B_2 , which may be calculated from the PMF via:

$$B_2 = 2\pi \int (1 - \exp(-\beta\psi(r))) r^2 dr \quad (8)$$

Positive values for B_2 indicate an overall repulsive force acting between the molecules; negative values indicate an overall attractive force.

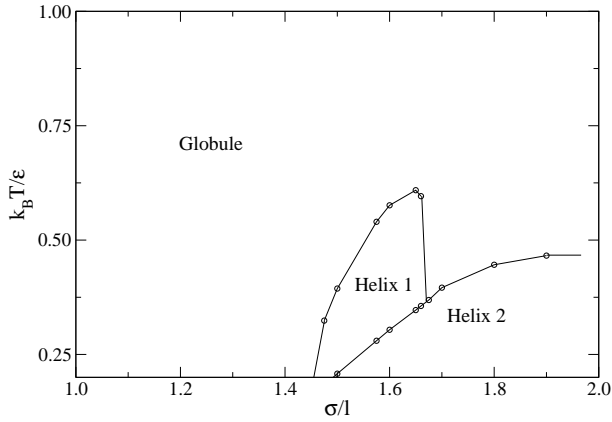


Figure 1: Single molecule phase diagram.

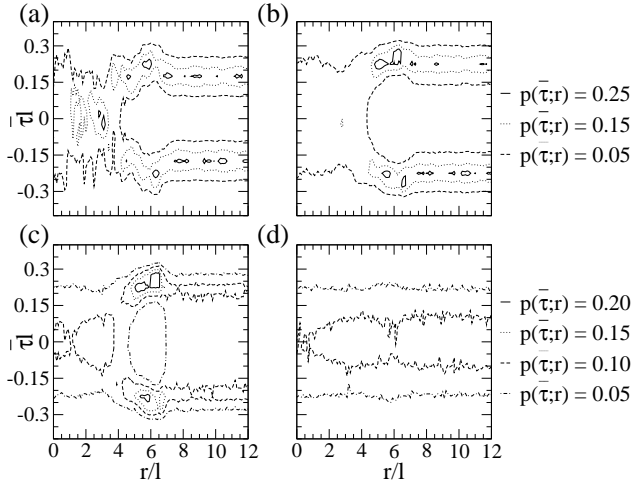


Figure 2: Contour plots of the estimated probability distributions $p(\bar{\tau}; r)$ for $\sigma/l = 1.6$ at (a) $k_B T / \epsilon = 0.255$, (b) $k_B T / \epsilon = 0.435$, (c) $k_B T / \epsilon = 0.651$, and (d) $k_B T / \epsilon = 1.164$.

III. RESULTS AND DISCUSSION

In previous work,¹⁹ we have studied this polymer model for isolated 20mers, down to a temperature of $k_B T / \epsilon = 0.2$. It was found that, at sufficiently low temperatures, these polymers may form helical structures, depending upon the value for σ/l . Further, two separate helical phases were observed over the range $1.475 \leq \sigma/l \leq 1.66$. For reference, the phase diagram of the single polymer system is reproduced in Fig. 1. In this work, we study the behavior of an isolated pair of polymer molecules with $\sigma/l = 1.3$, 1.6 and 1.9 .

A. $\sigma/l = 1.6$

We begin with a description of the results for the $\sigma/l = 1.6$ system, which best demonstrates behaviors which also occur in the $\sigma/l = 1.3$ and $\sigma/l = 1.9$ systems. Results are presented across a range of separations at four representative temperatures; $k_B T / \epsilon = 0.255$, for which isolated polymers are in the helix 2 phase, $k_B T / \epsilon = 0.435$, for which isolated polymers are in the helix 1 phase, $k_B T / \epsilon = 0.651$, just above the helix 1-globule transition temperature, and $k_B T / \epsilon = 1.164$, at which the polymer is well into the globule phase.

In order to illustrate the structural behavior of the interacting molecules, contour plots of $p(\bar{\tau}; r)$ against r are displayed in Fig. 2. The thermodynamic behavior is shown in Fig. 3. The potential of mean force is given in Fig. 3(a), the mean intramolecular interaction energy $\langle E_{intra} \rangle$ is given in Fig. 3(b), and the variation of the intermolecular interaction energy $\langle E_{inter} \rangle$ is given in Fig. 3(c). The correlations between the intramolecular energies $\text{cor}(E_1, E_2)$,

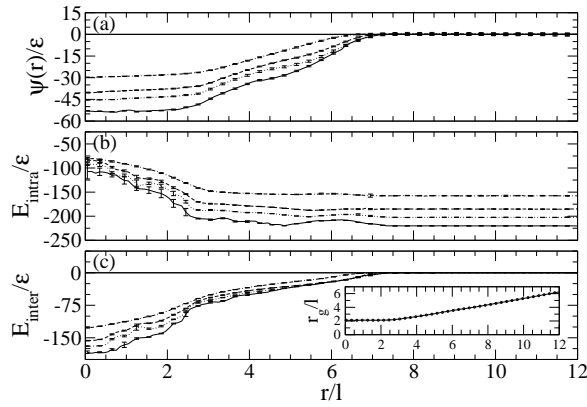


Figure 3: Variation of thermodynamic properties with molecular separation for $\sigma/l = 1.6$: (a) potential of mean force, (b) intramolecular interaction energy, and (c) intermolecular interaction energy. Solid lines denote $k_BT/\epsilon = 0.255$, dotted lines denote $k_BT/\epsilon = 0.435$, dashed lines denote $k_BT/\epsilon = 0.651$, and dot-dashed lines denote $k_BT/\epsilon = 1.164$. Inset: Root mean square radius of gyration r_g/l for $k_BT/\epsilon = 0.255$. Errors are less than symbol size. Equivalent data at higher temperatures are indistinguishable at this scale.

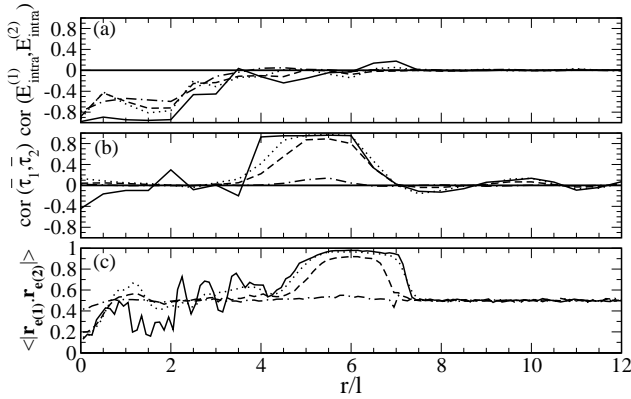


Figure 4: Intermolecular correlations for $\sigma/l = 1.6$ between: (a) intramolecular energies, (b) conformational torsions, and (c) end-to-end bond vectors. Solid lines denote $k_BT/\epsilon = 0.255$, dotted lines denote $k_BT/\epsilon = 0.435$, dashed lines denote $k_BT/\epsilon = 0.651$, and dot-dashed lines denote $k_BT/\epsilon = 1.164$.

the mean torsions $\text{cor}(\bar{\tau}_1, \bar{\tau}_2)$, and the orientation of the end-to-end distance vectors $\langle \mathbf{r}_{e(1)} \cdot \mathbf{r}_{e(2)} \rangle$, for the molecules are shown in Fig. 4.

The lowest representative temperature ($k_BT/\epsilon = 0.255$) is less than the helix 1-helix 2 transition temperature, and the results are typical of this region. In Fig. 2(a), it can be seen that at separations $r/l \gtrsim 7.5$, $p(\bar{\tau}; r)$ is independent of r , bimodal and approximately zero at $\bar{\tau} = 0$. In Fig. 3 (solid line), it can be seen that, at these large separations, $\psi(r)$ and $\langle E_{intra} \rangle$ are approximately zero, and $\langle E_{inter} \rangle$ appears r -independent. Finally, as shown in Fig. 4 (solid line), all three measured correlators are approximately zero for large separations. This behavior indicates that, for $r/l \gtrsim 7.5$, the two molecules do not significantly interact with each other, existing independently in the helix 2 state. There is a weak interaction, since observed $\langle E_{inter} \rangle$ is non-zero, with magnitude greater than observed error, for $r/l \lesssim 8.5$; however, these interactions do not appear strong enough to significantly perturb the isolated equilibrium state.

The interactions between the molecules begin to perturb their individual structures at $r/l \approx 7.5$. In the range $4 \lesssim r/l \lesssim 7.5$, $p(\bar{\tau}; r)$ remains bimodal, however, the positions of the peaks, $\pm \bar{\tau}_{max}$ depend upon separation. As shown in Fig. 3, over the same range, $\psi(r)$ and $\langle E_{intra} \rangle$ are monotonically increasing functions of r , while $\langle E_{inter} \rangle$ remains approximately constant. Further, the torsions and end-to-end vectors of the molecules become strongly correlated in this region, while intramolecular energies remain uncorrelated (see Fig. 4).

The bimodality of the torsion distributions, as well as the approximately constant value for the intramolecular energies, indicates that the molecules maintain helical configurations within this range. A snapshot configuration of two helical molecules taken at this temperature is presented in Fig. 5(a). The observed correlations show that the helices have a strong preference to take on the same handedness, and lie end-to-end along the same axis.

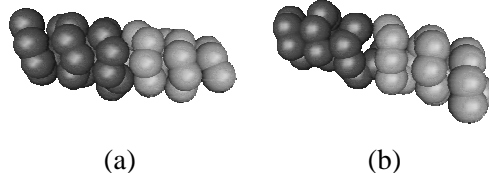


Figure 5: Snapshot configuration for (a) $\sigma/l = 1.6$, $k_BT/\epsilon = 0.255$, umbrella potential centered at $b/l = 5$, and (b) $\sigma/l = 1.6$, $k_BT/\epsilon = 0.651$, umbrella potential centered at $b/l = 5.6$.

The average end-to-end distance for the unperturbed polymer at this temperature¹⁹ is $r_e/l \approx 5$; two completely rigid “average” helices would only begin to interact at $r/l = 5.5$. For two helices to interact at $r/l = 7.5$, they must have $r_e/l > 7$, which corresponds to an extension of at least 27%. The interactions between the molecules appear to stretch the molecules, relative to their isolated equilibria.

The stretching effect weakens upon closer approach between the molecules; at separations $4 \lesssim r/l \lesssim 5$, $\bar{\tau}_{max}$ approximately returns to its value at large separation. Further, $\langle |\mathbf{r}_{e(1)} \cdot \mathbf{r}_{e(2)}| \rangle$ decreases to approximately 0.5 at separations in this range, indicating that the two molecules are less likely to align. For an isolated molecule at this temperature, $r_e/l \approx 5$; for two aligned “average” helices, there would be a longitudinal compression at separations closer than this. As such, the stretching force is eliminated, and in order to remain helical, the helical axes must lose some orientational correlation upon further approach. Note that the torsion correlator remains high across this region. In the range $4 \lesssim r/l \lesssim 7.5$, the intramolecular energies of the two molecules are uncorrelated.

Once the two molecules approach closer than $r/l \approx 4$, $p(\bar{\tau}; r)$ becomes unimodal (see Fig. 2); that is, the structures become achiral, and helicity is lost. This behavior is marked by a small discontinuity in total energy (data not shown) at $r/l = 4.15$ and a sudden loss of torsional correlations between the molecules. For $2.5 \lesssim r/l \lesssim 4$, $\psi(r)$ and $\langle E_{inter} \rangle$ increase monotonically with r , $\langle E_{intra} \rangle$ remains approximately constant, and no significant correlation exists between the intramolecular energies. The intermolecular interactions in this range are strong enough to fully disrupt the helical structures, causing both molecules to adopt individual unstructured globule configurations. We suggest that the lack of intramolecular energy correlations and the approximately constant intramolecular energy indicate that, at these separations, the complex consists of two globules with only limited interpenetration. The steady decrease in $\langle E_{inter} \rangle$ with decreasing r suggests that the two globules deform upon approach to give a larger contacting interface.

At $r/l = 2.5$, however, there is a large discontinuity in $\langle E_{inter} \rangle$ and in $\langle E_{intra} \rangle$. Further, the slope of $\langle E_{intra} \rangle$ versus separation changes at this separation; for $r/l > 2.5$, the average intramolecular energy is approximately constant (with respect to r), however, for $r/l < 2.5$, it is a decreasing function of r . For $r < 2.5$, there is a negative correlation between the intramolecular energies. This shift has no obvious signature in $p(\bar{\tau}; r)$. The inset to Fig. 3 shows that, below $r/l \approx 2.5$, the radius of gyration of the system becomes approximately constant ($r_g/l \approx 2.1$); further approach does not lead to contraction of the complex. The *total* energy of the system (i.e., $E = E_{intra} + E_{inter}$) also becomes approximately constant with respect to r at these short separations (data not shown). This suggests increasing interpenetration between the two molecules, with intramolecular contacts being replaced on a one-to-one basis by intermolecular contacts. Since $\psi(r)$ is also approximately constant for $r/l < 2.5$, this implies that the entropy of the system also remains approximately constant at these separations. Strong anticorrelation of intramolecular energies, indicated by large negative values for $\text{corr}(E_1, E_2)$, shows that any “swelling” (loss of intramolecular contacts) of one molecule must be matched by an equivalent “collapse” (gain in intramolecular contacts) of the other. These data are consistent with two interpenetrated molecules in a collapsed, unstructured globule state.

It is unclear why, for separations $2.5 < r/l \lesssim 4$, the two molecules act like immiscible droplets, whereas for $r/l < 2.5$, the molecules can interpenetrate; nor is it clear why the transition between the two is so sharp.

Qualitatively similar behavior is seen when $k_BT/\epsilon = 0.435$, which is in (and typical of) the helix 1 phase for an isolated polymer. Once again, at large separations, molecules adopt two independent, uncorrelated helical structures. Upon closer approach, interactions once again cause correlation between the helical axis and torsions and cause stretching forces which lead to extended helical configurations. Closer still, correlations and helical structure are suddenly lost, and the system appears to form two contacting but distinct unstructured globules. Finally, interactions cause the two molecules to interpenetrate, forming a single globule, which again is marked by a broad, flat minimum in $\psi(r)$.

Increasing the temperature to $k_BT/\epsilon = 0.651$, there is unexpected behavior. This temperature is above that of the helix 1-globule transition, and, consequently, at large separations the molecules adopt unstructured globule configurations, with no chiral symmetry breaking. However, at $r/l = 6.8$, there is a small discontinuity in the total energy (not shown), and $p(\bar{\tau}; r)$ changes from a broad, unimodal distribution to a bimodal distribution. That is, upon approach, interactions between the two molecules cause chiral symmetry breaking and helix formation, at a

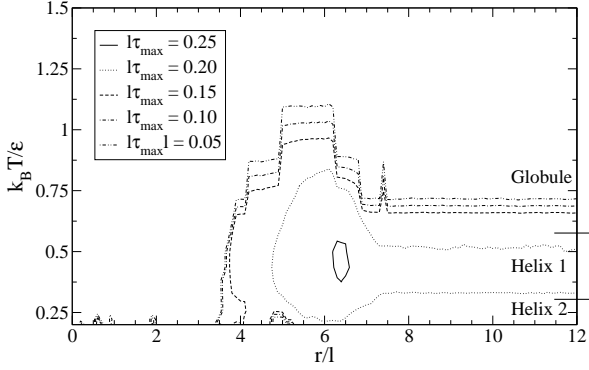


Figure 6: Contour plot of the absolute mode $\bar{\tau}_{max}$ of $p(\bar{\tau}; r, T)$ for $\sigma/l = 1.6$. The positions of the globule - helix 1 and helix 1 - helix 2 transitions are marked on the right hand side. Note that non-zero $\bar{\tau}_{max}$ is not sufficient for chiral symmetry breaking; see discussion in Section II and Ref. 19.

temperature above that where helical configurations would normally be stable. A snapshot configuration is shown in Fig. 5(b). The character of this pair of helices is very similar to the helices seen for the same separations at lower temperatures (see Fig. 5(a)), with similar torsion values and correlation in helical axes and torsions. We suggest that attractive intermolecular interactions between the globules produce a stretching force, which has previously been shown to stabilize helix formation.²⁹ As the two molecules continue to approach each other, there is once again a loss of helical structure and intermolecular correlations to two unmixed globules, followed by interpenetration and mixing.

Finally, consider the temperature $k_B T/\epsilon = 1.164$, which is above that of the helix-globule transition for isolated polymers. The torsion distribution $p(\bar{\tau}; r)$ exhibits a broad, unimodal structure for all separations; this system shows no chiral symmetry breaking, and no helix formation. There are no observed correlations between the torsions or the end-to-end vectors of the molecules. There is an apparent transition between separate and interpenetrated globules, marked by a slight discontinuity in total energy, changes in the slope of $\psi(r)$ and the inter- and intramolecular energies, and sudden onset of strong anticorrelations between intra-molecular energies. It is also interesting to note that the potential of mean force at this temperature is qualitatively similar to those for the lower temperatures; it appears that the presence or absence of helical structure has little effect on the character of the PMF.

A contour plot of $\bar{\tau}_{max}$ as a function of $k_B T/\epsilon$ and r is shown in Fig. 6. Note that regions of non-zero $\bar{\tau}_{max}$ do not necessarily indicate helical configurations; as pointed out in our previous work¹⁹ for single molecules, there exists a region just above the helix transition where $p(\bar{\tau})$ is double peaked but has a non-zero value around $\bar{\tau} = 0$, and as such is not truly symmetry breaking. However, this contour plot does schematically show the increase in stability of helical structures at intermediate separations, as well as the loss of helical structure at close separation.

B. $\sigma/l = 1.9$

Potential, torsion and correlation data for the $\sigma/l = 1.9$ system are shown in Figs. 7, 8 and 9. A plot of $\bar{\tau}_{max}$ against separation and temperature is shown in Fig. 10. Once again, we consider representative temperatures: this time, $k_B T/\epsilon = 0.651$, typical of the region just above the helix 2 - globule and $k_B T/\epsilon = 1.455$, typical of higher temperatures. We were not able to fully equilibrate the two molecules at temperatures below the helix 2 - globule transition.

The behavior at the lower temperature $k_B T/\epsilon = 0.651$ is qualitatively similar to the situation for the $\sigma/l = 1.6$ system at $k_B T/\epsilon = 0.651$. The torsion histograms in Fig. 8(a) reveal a range of separations over which helical structures are observed at temperatures higher than found for isolated molecules. This range is associated with a correlation between the torsions of the two molecules (Fig. 9(b), solid line), although this correlation is not as strong as that observed for the $\sigma/l = 1.6$ system. Interestingly, there is no significant correlation in the end-to-end bond vectors over this range (Fig. 9(c), solid line). At close separations, the intramolecular energies of the two molecules become strongly anticorrelated (Fig. 9(a), solid line). This correlation appears gradually on approach from the loss of helical structure (at $r/l \approx 4$) to a discontinuity in intramolecular and intermolecular energies (at $r/l = 2.4$). Once again, this separation coincides with the point at which the radius of gyration (not shown) becomes approximately constant, with $r_g/l \approx 2.4$, and below this separation, total energy and $\psi(r)$ (Fig. 7(a), solid line) are also independent of r . Aside from the lack of orientational correlation, the only other qualitative difference is a repulsive “hump” in $\psi(r)$ at long ranges for the $\sigma/l = 1.9$ system. The maximum of this barrier ($r/l = 8.25$) is near to the separation

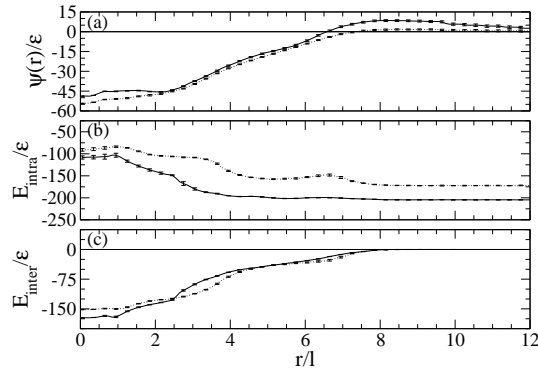


Figure 7: Variation of thermodynamic properties with molecular separation for $\sigma/l = 1.9$: (a) potential of mean force, (b) intramolecular interaction energy, and (c) intermolecular interaction energy. Solid lines denote $k_BT/\epsilon = 0.651$ and dotted lines denote $k_BT/\epsilon = 1.455$.

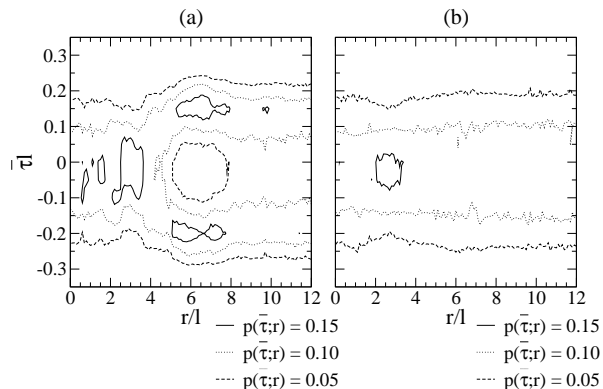


Figure 8: Contour plots of the estimated probability distributions $p(\bar{\tau}; r)$ for $\sigma/l = 1.9$ at (a) $k_BT/\epsilon = 0.651$, and (b) $k_BT/\epsilon = 1.455$.

at which $\langle E_{\text{inter}} \rangle$ becomes non-zero — this barrier is, therefore, entropic in nature, corresponding to loss of entropy of extended configurations. The long range of this hump suggests that such extended configurations are relatively frequent occurrences — this is to be expected, considering the stiffness of the $\sigma/l = 1.9$ polymer. Overall, then, the results are consistent with the interpretations offered for the $\sigma/l = 1.6$ system at the same temperature.

At $k_BT/\epsilon = 1.455$, there is new behavior. While the torsional behavior (Fig. 8(b)), potential of mean force and energies (Fig. 7, dotted line), and the torsional and end-to-end vector correlators (Fig. 9(b) (c), dotted line) appear

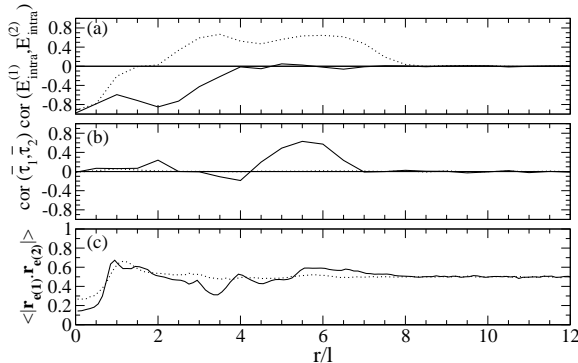


Figure 9: Intermolecular correlations for $\sigma/l = 1.9$ between: (a) intramolecular energies, (b) conformational torsions, and (c) end-to-end bond vectors. Solid lines denote $k_BT/\epsilon = 0.651$, dotted lines denote $k_BT/\epsilon = 1.455$.

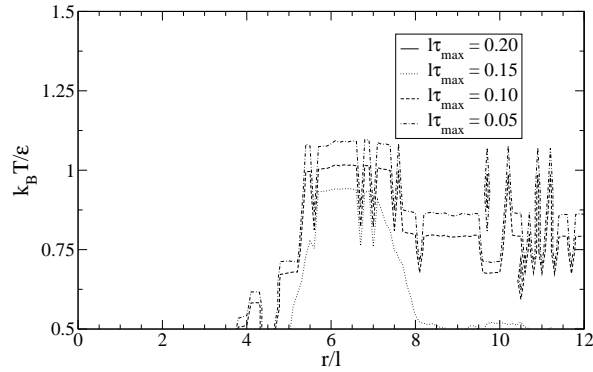


Figure 10: Contour plot of the absolute mode τ_{max} of $p(\bar{\tau}; r)$ for $\sigma/l = 1.9$. All temperatures shown are above the helix 2 - globule transition temperature.

similar to those seen at high temperatures for $\sigma/l = 1.6$, there are strong internal energy correlations across the range $2 \lesssim r \lesssim 8$ (Fig. 9(a), dotted line). These correlations are observed at temperatures up to $k_B T/\epsilon = 2.273$ - above this, the system returns to the qualitative behavior seen for $\sigma/l = 1.6$, $k_B T/\epsilon = 1.164$. Snapshot configurations taken across this range of temperature and separation do not show any remarkable common features; the system appears to be exploring a large ensemble of unstructured configurations.

The positive intramolecular energy correlation indicates that swelling of one polymer is associated with swelling of the other. We relate this to the stretching force that we have inferred to operate between helices over a similar range of separations. If one of the polymers is in a particularly open (high intramolecular energy) configuration, then it will have a larger radius. This will increase the likelihood of interactions with the other polymer; if these interactions are attractive, then the other polymer can only expand (at fixed intermolecular separation). The variance in intramolecular energies for the $\sigma/l = 1.9$ system in the globule phase is approximately double that observed for the $\sigma/l = 1.6$ globule phase (data not shown). This indicates that the $\sigma/l = 1.9$ globule phase has much lower internal cohesion than the globules at smaller overlaps, which we suggest is due to the inherent stiffness of the polymer, and which allows cross interactions to produce these cross-correlations which are not observed for the $\sigma/l = 1.6$ system.

In summary, the behavior of the $\sigma/l = 1.9$ system is largely similar to that of the $\sigma/l = 1.6$ system, with destruction of helical structure at short range, stabilization of helical structure at intermediate range, and an apparent transition between separate and interpenetrated globules at very close range. A summary of the torsional behavior of the system is shown in Fig. 10. Two significant differences in behavior occur. First, strong correlations in intramolecular energies between the two molecules are observed in the unstructured globule phase. We suggest that this does not occur in the $\sigma/l = 1.6$ system because the individual globules are more internally cohesive, as indicated by lower intramolecular energy fluctuations. Further, no correlations between the end-to-end bond vectors of the helices are observed; we will return to this point in the conclusion.

C. $\sigma/l = 1.3$

Finally, consider square-well polymers with $\sigma/l = 1.3$. Here, we present two representative temperatures, $k_B T/\epsilon = 0.255$ and $k_B T/\epsilon = 0.651$. Single 20mers with $\sigma/l = 1.3$ do not display¹⁹ any helical structure down to a temperature of $k_B T/\epsilon = 0.2$. Potential of mean force and energies are shown in Fig. 11, contour plots of $p(\bar{\tau}; r)$ in Fig. 12, and correlations in Fig. 13.

At the lower temperature $k_B T/\epsilon = 0.255$, the behavior is similar to that seen for the $\sigma/l = 1.6$ and $\sigma/l = 1.9$ systems at temperatures just above the helix-globule transition. At long range, there is no torsional symmetry breaking. This continues on approach down to $r/l = 5.65$, where there is a sudden discontinuity in intramolecular and intermolecular energies. At this separation, $p(\bar{\tau}; r)$ abruptly becomes bimodal, and the torsions and end-to-end vectors become strongly correlated. This behavior indicates that the helix phase is stabilized by interactions between the polymers. This stability continues across the range $3.65 \lesssim r/l \lesssim 5.65$. At $r/l = 3.6$, there is a small discontinuity in the total energy, the torsion histogram is no longer bimodal, and the torsions and orientations of the molecules are no longer correlated. At closer separations, there is a gradual increase in anticorrelation between the intramolecular energies up to a discontinuity in intermolecular energy at $r/l = 1.8$. Upon closer approach, the intramolecular energies are strongly anticorrelated, and the PMF and total system r_g remain approximately constant. This behavior is once again interpreted as a transition from two immiscible polymer globules at intermediate separation to two interpenetrating

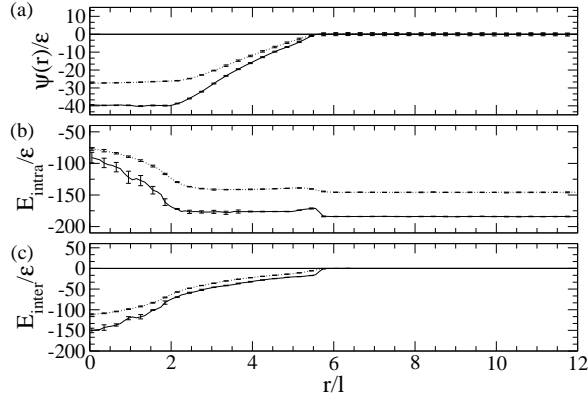


Figure 11: Variation of thermodynamic properties with intermolecular separation for $\sigma/l = 1.3$: (a) potential of mean force, (b) intramolecular interaction energy, and (c) intermolecular interaction energy. Solid lines denote $k_BT/\epsilon = 0.255$, and dotted lines denote $k_BT/\epsilon = 0.651$.

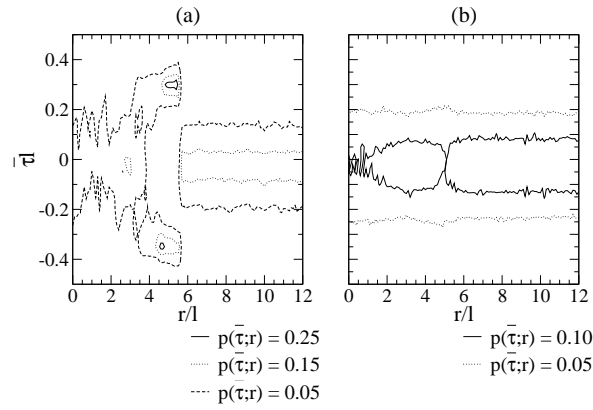


Figure 12: Contour plots of the estimated probability distributions $p(\bar{\tau};r)$ for $\sigma/l = 1.3$ at (a) $k_BT/\epsilon = 0.255$, and (b) $k_BT/\epsilon = 0.651$.

globules at close separations.

At the higher temperature $k_BT/\epsilon = 0.651$, the behavior is similar to that seen for the $\sigma/l = 1.6$ and $\sigma/l = 1.9$ systems in the unstructured globule regime. The torsions and end-to-end vectors remain uncorrelated at all separations, and the torsion histograms remain unimodal. The mixing transition between the two globules appears at close separation, marked by the onset of intramolecular energy correlations. No strong intramolecular energy correlations are observed. The variance in the intramolecular energies is of the order of magnitude of that seen for the $\sigma/l = 1.6$ system, which suggests that the globules have enough internal cohesion to prevent such correlation.

The torsional data are summarized in Fig. 14 and are similar to the data presented in Figs. 6 and 10 for temperatures above the helix-globule transition.

D. Summary

In summary, we have found similar behaviors for pairs of model polymers for $\sigma/l = 1.3$, 1.6 and 1.9. In each case, intermediate separations between the molecules enhance helix stability, showing paired helical configurations at temperatures above the single molecule helix-globule transition temperature. For these separations, the paired helices have strongly correlated chiralities, and for $\sigma/l = 1.3$ and 1.6, are aligned end-to-end. At separations closer than the typical helix length, however, the molecules lose helicity and adopt disordered configurations. At separations immediately below the typical helix length, the disordered globular configurations of the polymers are uncorrelated. As the separation becomes approximately equal to the radius of gyration of the complex, however, energy anticorrelations begin to develop between the two molecules; below this separation, the radius of gyration of the complex remains approximately constant. The potential of mean force is qualitatively insensitive to σ/l , consisting of a monotonically

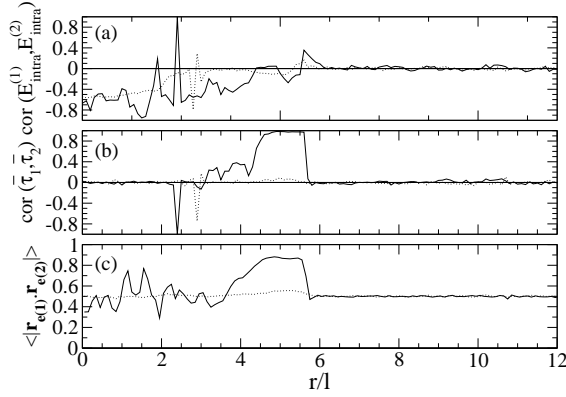


Figure 13: Intermolecular correlations for $\sigma/l = 1.3$ between: (a) intramolecular energies, (b) conformational torsions, and (c) end-to-end bond vectors. Solid lines denote $k_B T/\epsilon = 0.255$; dotted lines denote $k_B T/\epsilon = 0.651$.

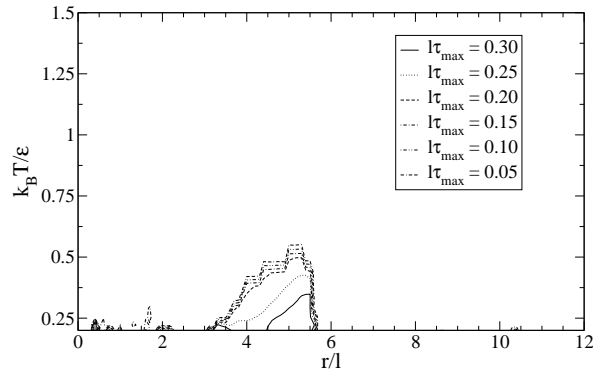


Figure 14: Contour plot of the absolute mode τ_{max} of $p(\bar{\tau}; r)$ for $\sigma/l = 1.6$.

decreasing “ramp” from the initial onset of interactions at large separations, down to the separation at which energy correlations begin to occur between globules. Below this separation, the PMF remains approximately constant in a broad, flat minimum to zero separation. For the temperatures at which helical configurations are observed, the PMF’s are all strongly attractive, as evidenced by very large negative values for the second virial coefficient B_2 , shown in Fig. 15.

We suggest that the stabilization of helical structure at moderate separation occurs because attractive interactions between the two molecules exert a stretching force. Stretching forces have been shown to stabilize helix formation in other simple helix-forming models.²⁹ Correlation in chirality and helical axis can be seen as a consequence of

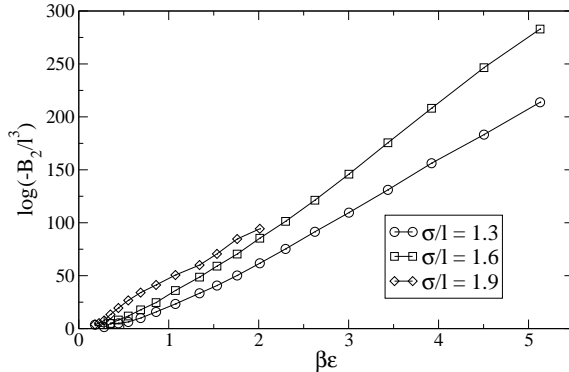


Figure 15: Log-reciprocal plot of minus the second virial coefficient, $-B_2/l^3$ against temperature, $k_B T/\epsilon$ for the three values of σ/l studied. Errors are smaller than symbol size.

energy minimization. By sampling face-to-face configurations, contacts between helices are possible at intermediate separation; by having the same chiralities, the match-up between the faces, and hence the number of contacts, is maximized. For $\sigma/l = 1.9$, there is no significant axial alignment, but there is a strong correlation in chirality between helices. This suggests that face-to-face interactions are strong enough to promote identical chirality between molecules even when such interactions are not strong enough to hold the two polymers in axial alignment.

IV. CONCLUSIONS

The observed behaviors are similar to those seen in simulations of helical homopolypeptides⁶ up to the separation at which helical structure is lost. Upon close approach, simulated homopolypeptides are observed to switch to parallel paired helical configurations, whereas for the simple model presented here, the system prefers to collapse into an unstructured globule. The helical structures which the system exhibits are simply not stable enough to overcome the free energy to be gained by formation of the collapsed structure.

One may therefore ask how the helix can be stabilized against the collapsed, disordered globule. We consider that the Θ -point of a polymer (the temperature at which $B_2 = 0$) is related to the gas-liquid transition in a bulk system. The Θ -point is also the temperature below which a single polymer will begin to collapse from an extended, disordered coil state (analogous to a gas) to a collapsed, disordered globule state (analogous to a liquid). If we hypothesize that the helical configuration is analogous to a bulk crystalline phase for the polymer model (since it is an ordered state which must be reached through a first-order transition), then we can consider methods by which the crystalline phase may be stabilized against the liquid phase. It has been shown^{30,31} that, for bulk systems of particles interacting via a simple, isotropic potential, decreasing the range of the attractive part of the potential can decrease the stability of the liquid phase to the point of leaving the liquid-gas critical point metastable with respect to the crystal phase. In analogy, we suggest that by decreasing λ in Eq. (1), we may depress the Θ -point of the system without depressing the helix transition temperature, so that the stability of the dense globule may decrease to the point that the observed collapse may not occur, giving results closer to those from simulations of homopolypeptides.

This suggestion may have a basis in the chemistry of real homopolypeptides. The strongest interaction present for these molecules is likely to be hydrogen bonding between segments of the peptide backbone. This hydrogen bonding is very strongly anisotropic, occurring for only a small range of orientational alignments between peptide segments. It has been shown that for bulk systems interacting via simple anisotropic potentials, decreasing the range of orientations over which interactions can occur depresses the temperature of the liquid-gas critical point.³²

We also observe that moderate proximity between pairs of square well homopolymers can promote the stability of helical structures. We have suggested that this may be linked to the stabilization of helical structure upon stretching of a single molecule, observed for other simple helix-forming models.²⁹ For pairs of molecules, this stabilization is not enough to prevent collapse into an unstructured globule. Experimentally, helix forming proteins aggregate to form ordered structures with molecules in aligned, extended configurations. Since such configurations are not seen for this model nor for simulations using pairs of more detailed model peptides,⁶ it seems that they must be stabilized by three or more body interactions between molecules. This suggests that bulk simulations using the model presented here may be useful.

In conclusion, we have shown that interactions between pairs of square well homopolymers can promote helix stability, while at close proximity, interactions cause collapse from paired helices to a single disordered globule. We have further suggested a modification to the model (a reduction in the range of the attractive part of the potential) which may stabilize the helix phase against such collapse, in order to provide better qualitative agreement with simulations of pairs of helix forming homopolypeptides. Finally, we have suggested that the reason for the formation of amyloid aggregate structures may lie in many-body interactions between molecules. These results underline the need for a better understanding of the underlying nature of the helix-disordered globule transition, in order to gain an understanding of how interactions between molecules can increase or decrease the relative stabilities of the various structures.

Acknowledgments

This work is supported by the EPSRC (grant reference EP/D002753/1).

¹ E. Chi, S. Krishnan, T. Randolph, and J. Carpenter, *Pharm. Res.* **20**, 1325 (2003).

- ² I. Baskakov, G. Legname, S. Prusiner, and F. Cohen, *J. Biol. Chem.* **276**, 19687 (2001).
- ³ W. Dzwolak, T. Muraki, M. Kato, and Y. Taniguchi, *Biopolymers* **73**, 463 (2004).
- ⁴ M. Fandrich and C. Dobson, *EMBO J.* **21**, 5682 (2002).
- ⁵ R. Armen, B. Bernard, R. Day, D. Alonso, and V. Daggett, *PNAS* **102**, 13433 (2005).
- ⁶ R. Curtis, R. Pophale, and M. Deem, *Fluid Phase Equilibria* **241**, 354 (2006).
- ⁷ S. Kim and D. Weaver, *J. Mol. Struct. - Theo. Chem.* **127**, 527 (2000).
- ⁸ T. Klein and C. Huang, *Biopolymers* **49**, 167 (1999).
- ⁹ M. Yang, M. Lei, and S. Huo, *Prot. Sci.* **12**, 1222 (2003).
- ¹⁰ A. Smith and C. Hall, *Proteins* **44**, 344 (2001).
- ¹¹ A. Smith and C. Hall, *Proteins* **44**, 376 (2001).
- ¹² A. Smith and C. Hall, *J. Mol. Biol.* **312**, 187 (2001).
- ¹³ H. Nguyen and C. Hall, *Biophys. J.* **97**, 4122 (2004).
- ¹⁴ A. Maritan, C. Micheletti, A. Trovato, and J. Banavar, *Nature* **406**, 287 (2000).
- ¹⁵ D. Marenduzzo, A. Flammmini, A. Trovato, J. Banavar, and A. Maritan, *J. Pol. Sci. B* **43**, 650 (2005).
- ¹⁶ A. Buhot and A. Halperin, *Macromolecules* **35**, 3238 (2002).
- ¹⁷ M. Muthukumar, *J. Chem. Phys.* **104**, 691 (1996).
- ¹⁸ V. Varshney, T. E. Dirama, T. Z. Sen, and G. A. Carri, *Macromolecules* **37**, 8794 (2004).
- ¹⁹ J. Magee, V. Vasquez, and L. Lue, *Phys. Rev. Lett.* **96**, 207802 (2006).
- ²⁰ Y. Zhou, C. Hall, and M. Karplus, *Phys. Rev. Lett.* **77**, 2822 (1996).
- ²¹ Y. Zhou, M. Karplus, J. Wichert, and C. Hall, *J. Chem. Phys.* **107**, 10691 (1997).
- ²² J. Magee, J. Warwicker, and L. Lue, *J. Chem. Phys.* **120**, 11285 (2004).
- ²³ J. Dautenhahn and C. Hall, *Macromolecules* **27**, 5399 (1994).
- ²⁴ A. Striolo and J. Prausnitz, *J. Chem. Phys.* **113**, 2927 (2000).
- ²⁵ A. Striolo, D. Bratko, and J. Prausnitz, *Polymer* **43**, 591 (2002).
- ²⁶ J. Wichert and C. Hall, *Macromolecules* **27**, 2744 (1994).
- ²⁷ C. Bokis, M. Donohue, and C. Hall, *Ind. Eng. Chem. Res.* **33**, 146 (1994).
- ²⁸ A. Maritan, C. Micheletti, A. Trovato, and J. Banavar, *Nature* **406**, 287 (2000).
- ²⁹ D. Marenduzzo, A. Maritan, A. Rosa, and F. Seno, *Phys. Rev. Lett.* **90**, 088301 (2003).
- ³⁰ A. Gast, C. Hall, and W. Russel, *J. Colloid Interface Sci.* **96**, 251 (1983).
- ³¹ S. Illet, A. Orrock, W. Poon, and P. Pusey, *Phys. Rev. E* **51**, 1344 (1995).
- ³² N. Kern and D. Frenkel, *J. Chem. Phys.* **118**, 9882 (2003).